Journal of Physics: Conference Series

PAPER • OPEN ACCESS

A blind test on wind turbine wake modelling based on wind tunnel experiments: Phase I – The benchmark case

To cite this article: V Pappa *et al* 2024 *J. Phys.: Conf. Ser.* **2767** 092053

View the article online for updates and enhancements.

You may also like

- Combining *in situ* tribometry and triboscopy to understand third body behavior of a Cd coating
P Behera, K R Sriraman, R R Chromik et al.
- Analyzing single-lead short ECG recordings using dense convolutional neural networks and feature-based post-processing to detect atrial fibrillation
Saman Parvaneh, Jonathan Rubin, Asif Rahman et al.
- Estimating the Milky Way's Mass via Hierarchical Bayes: A Blind Test on MUGS2 Simulated Galaxies
Gwendolyn Eadie, Benjamin Keller and William E. Harris

This content was downloaded from IP address 131.175.148.48 on 21/06/2024 at 10:19

Journal of Physics: Conference Series **2767** (2024) 092053 doi:10.1088/1742-6596/2767/9/092053

A blind test on wind turbine wake modelling based on wind tunnel experiments: Phase I – The benchmark case

V Pappa[a], F Campagnolo[b], S Tamaro[b], F Mühle[b], J Stegmüller[f], A Croce[c], C Gromke[d], V Riziotis[a], C Bottasso[b], A Sciacchitano[e], D Bouris[a] and M Manolesos[a]

[a]School of Mechanical Engineering, National Technical University of Athens, Iron Politechniou 9, 15780, Athens, Greece
[b]Wind Energy Institute, Technical University of Munich, Boltzmannstr. 15, 85748, Munich, Germany
[c] Department of Aerospace Engineering, Politecnico di Milano, Piazza Leonardo da Vinci, 32, 20133, Milano, Italy
[d]Karlsruhe Institute of Technology, Institute for Hydromechanics, Kaiserstr.12, 76131, Karlsruhe, Germany
[e]Delft University of Technology, Aerospace Engineering, Mekelweg 5, 2628 CD, Delft, the Netherlands
[f]Chair of Aerodynamics and Fluid Mechanics, Technical University of Munich, Boltzmannstr. 15, 85748, Munich, Germany

marinos@fluid.mech.ntua.gr

Abstract. Wind turbine wake and modelling is crucial to optimizing future wind farm layouts and hence reducing the cost of energy. This paper presents the first phase of a blind test on modelling controlled and uncontrolled wind turbine wakes. The blind test is based on wind tunnel experiments of two model scale wind turbines (D = 1.1 m) one downstream of the other. The exercise is split into two phases and the first one is presented here, where participants are invited to simulate the baseline case, in which both turbines are aligned with the flow and there is no control on the either turbine. The objective of this phase is to ensure all participants can benchmark their numerical approach against a baseline open data set, where no wake control is applied. Experimental measurements include inflow velocity, turbine power and loads for a range of tip speed ratios. In the second phase, not presented here, the wake of the upstream turbine will be controlled and the performance of the downstream one will be recorded. This will be a blind test with the data not released prior to submissions. The present paper gives an overview of the initial, open benchmark case, including its objectives, methodology and experimental results.

1. Introduction

As the wind energy sector continues to expand, the optimization of wind farm design and operation becomes increasingly critical. Central to this optimization is the accurate modeling of wind turbine

Content from this work may be used under the terms of the Creative Commons Attribution 4.0 licence. Any further distribution of this work must maintain attribution to the author(s) and the title of the work, journal citation and DOI.
Published under licence by IOP Publishing Ltd

wakes, as they can significantly impact energy production, turbine placement, and operational strategies within a wind farm. Wind turbine wake modeling, however, presents a scientific challenge due to the interplay of complex fluid dynamics, atmospheric boundary layer flow and the geometric layout of wind farms [1].

At the same time, effective wake control is a critical component of maximizing the energy potential of wind farms and accelerating the clean energy transition. By implementing wake control strategies, it is possible to significantly increase the energy production of a plant, and hence reduce the levelized cost of energy and increase wind farm economic viability. In order to select an optimal wake control strategy, accurate wake modelling is required [2].

In this context, the present paper introduces a blind test on wind turbine wake modelling and control based on scaled wind tunnel models. Building on the success of previous blind tests in the wind energy field [3], the present effort aims to serve as a collaborative endeavour, uniting researchers, engineers, and industry stakeholders to assess the capabilities of different modelling approaches. By subjecting these solvers to rigorous testing under controlled conditions and comparing their results to wind tunnel measurements, this initiative seeks to address fundamental questions in the field of wake modelling. At the same the component of individual pitch control for wake manipulation is added for the first time in such an exercise.

The motivation behind this endeavour is multifaceted. Firstly, it aims to validate the performance of numerical solvers, providing confidence in the tools used for wind farm design and optimization. Secondly, it fosters innovation by encouraging solver developers to enhance their algorithms and techniques. Moreover, the initiative promotes standardization by identifying best practices and methodologies that work effectively across a range of scenarios. Beyond these objectives, this and similar validation efforts help mitigate the financial risks associated with suboptimal wind farm layouts, support informed decision-making, and contribute to the advancement of scientific knowledge in wind energy.

This initiative is part of the TWEET-IE project, a Horizon Europe project on wind tunnel testing for energy and the environment. The blind test has been developed in collaboration with the Wake and Wind farm Aerodynamics Committee of the European Academy of Wind Energy.

1.1. The blind test

The blind test is split into two distinct phases. The first is an open-data benchmarking exercise, while the second is the actual blind test.

1.1.1. Phase I – The benchmark case

During the first phase, announced and commencing during the TORQUE 2024 conference, participants are invited to simulate the baseline case, where both turbines are aligned with the flow and there is no control on the either turbine. The objective of this phase is to enhance our understanding of wake and wake control modelling during the second phase, by eliminating teething issues with the modelling of the experiments in the first phase. This is done by ensuring all participants can benchmark their numerical approach against a baseline open data set, where no wake control is applied. All data for Phase I are publicly available here: DOI 10.5281/zenodo.10566400.

1.1.2. Phase II – Blind test

During the second phase, a more complex case will be considered, where the wake of the upstream turbine is controlled by means of active individual blade pitch. In this instance, only the case specification will be announced (inflow, wind turbine geometry, wind tunnel geometry, wake control strategy), without the results (performance of the two turbines). The objective of this phase is to benchmark different numerical approaches; quantify uncertainty; enhance confidence and trust in numerical techniques and drive relevant advancements.

The submitted results will be compared to the wind tunnel measurements to evaluate solver accuracy and reliability. To this end, clearly defined quantitative metrics will be used (e.g. turbine performance,

thrust, torque, vortex strength/development) and the suitability of the different approaches for different applications will be assessed. We intend to openly publish the blind test results to share the findings with the wind energy community in order to promote transparency, share best practice guidelines and help improve solver capabilities.

1.1.3. Schedule

Data for Phase I will become available in May 2024 and the details of the benchmarking campaign will be further detailed in a Webinar in June 2024. It is envisaged that submissions from participants will be collected in Winter 2024-2025 and the comparative results will be presented in Summer 2025. Phase II will be initiated in Winter 2025. All communications will be done through the project's website, http://www.tweet-ie.eu/.

1.2. Paper structure

The present paper is organized as follows. First the experimental set up is given, followed by the results and discussion. The paper closes with a concluding section. It is noted that this paper serves as an announcement of the Benchmark case, however, the published data will be accompanied by a detailed description of the measurement procedure, set up and results, which should be used to help set up numerical simulations.

2. Experimental set-up

2.1. Wind tunnel test section

All measurements were conducted in the closed-loop, low-speed boundary layer wind tunnel of the Chair of Aerodynamics and Fluid Mechanics at Technische Universität München (TUM). This wind tunnel has a test section of: 21m (L) x 2.7m (W) x 1.8m (H), as presented in Figure 1. The blower is driven by a 210 kW electric motor, which allows velocity regulation from 1 m/s to 30 m/s. More technical details about the wind tunnel can be found in [4].

Figure 1 presents the static pressure taps located at the centre of the wind tunnel ceiling. This is an adjustable ceiling that enables an approximately zero pressure gradient to be obtained along the wind tunnel test section. The pressure taps coordinates in the streamwise (x, cm) and vertical (z, cm) directions are shown in Figure 2. $\Delta P_{static\ (i)}$ is defined as the difference between static pressure at the ith tap (P_i) and atmospheric pressure (P_{atm}),

$$\Delta P_{static,i} = P_i - P_{atm} \quad (1)$$

The pressure measurements were recorded without and with wind turbine models within the test section for a time period of $t_{empty} = 5\ sec$.

The tunnel wind speed is measured with a Pitot tube in a distance of $4D$ upwind of the upstream wind turbine model (Figure 1). The pitot tube is located at hub height, 50cm from the tunnel side wall.

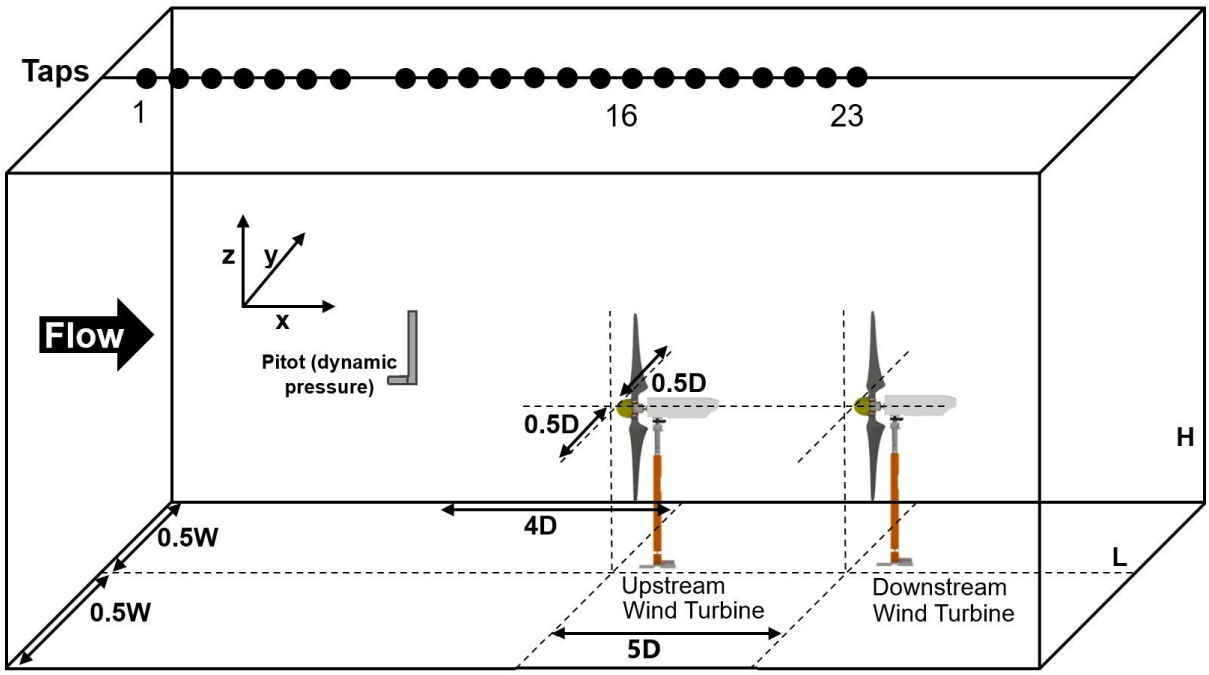

Figure 1. Sketch of the wind tunnel test section with the positioning of the pressure taps in the centre of the wind tunnel ceiling, the location of the pitot tube and the locations of the upstream and downstream wind turbine models.

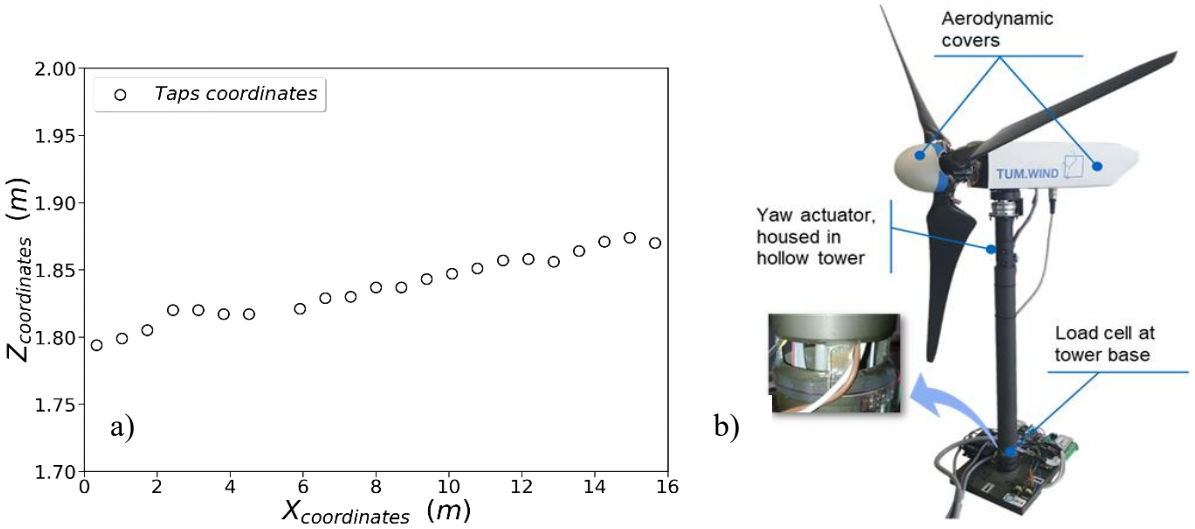

Figure 2. a) Streamwise (x, m) and vertical (z, m) coordinates of the pressure taps at different positions, along the centre of the wind tunnel ceiling; b) The G1 wind turbine with highlighted components.

2.2. Equipment

In addition to the sensors on the two wind turbine models a fast response aerodynamic probe (FRAP) was used to measure the velocity profiles at the locations of the two turbines and at the wake of the upstream one, when operating on its own. The probe was mounted on a traverse system to move between positions inside the test section.

The head of the FRAP probe is 3D printed, while its tip with a diameter of 3 mm is finished mechanically to guarantee small intrusivity. Pressure is measured by five differential piezo-resistive pressure sensors at the back of the probe head. Details about the probe and its application can be found in [5–7]. The FRAP is calibrated for its spatial and its temporal characteristics. The calibration allows for maximum flow angles of up to ±60°and sampling frequencies of up to 10 kHz. Within this operational range, FRAP can achieve high accuracies of 0.2° for both flow angles and 0.1 m/s for the reconstructed velocity.

2.3. Inflow velocity and turbulence intensity profiles

The inflow velocity profile was measured directly at two locations inside the empty test section: firstly, the velocity profile was recorded at the position of the upstream wind turbine and secondly at the corresponding position of the downstream wind turbine model, as presented in Figure 1. Both instantaneous velocity signals were measured at 14 points along a vertical line above the wind tunnel floor, without the turbine models in the test section. The velocity signal was sampled at 10 kHz for a total sampling time of 30s. Two main flow characteristics were determined: the mean wind velocity profile u(z) and the turbulence velocity profile TI_u (%), in the streamwise direction.

2.4. Wind Turbine Models

The wind turbine models used in the blind test, are the G1 turbines, developed by TUM. A detailed description of the turbine design and applications are presented [8–10] while a detailed picture of the G1 turbine can be seen in Figure 2. The G1 features a rotor diameter, D = 1.1 m, a hub height of $z_{hub} = 0.82m$ and has a rated rotor speed, ω = 850rpm (clockwise rotation). Chord and twist distributions are given in Figure 3.

The turbines are heavily equipped with sensors and multiple actuators including individual pitch, torque and yaw control. The turbine performance can be acquired by various sensors that measure the shaft loads, shaft torque, tower loads, blade pitch, turbine yaw and rotor azimuth. The turbine is controlled by a Bachmann PLC, similar to that of full-scale machines. The full set of airfoil profiles, chord and pitch distributions and profile polars is available online with the measurement data.

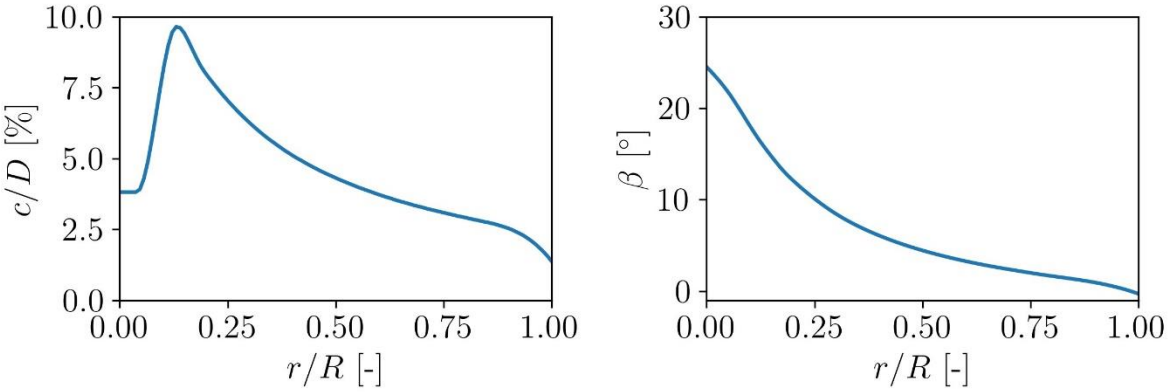

Figure 3. Chord and twist distribution for the G1 wind turbine model

2.5. Baseline scenarios

The Benchmark Case includes the aerodynamic performance characterization of two identical G1 wind turbine models when independently but also synchronously are placed in the wind tunnel test section. During the experimental procedure, when G1 wind turbine model is inserted in the test section, the wind tunnel blockage ratio $\alpha_{Block} = A_{turbine}/A_{tunnel}$, corresponds to α_{Block} = 20%. Blockage ratios of this order

have a significant influence on the wind turbine performance as well as the wake [11]. However, no blockage correction was applied to the data sets, taking into consideration that the computational modelers will be asked to include the wind tunnel walls in their simulations.

2.5.1. Individual Wind Turbines

The first phase of this experimental investigation includes the use of two identical G1 wind turbine models at the TUM test section, referred to as the upstream wind turbine model and the downstream wind turbine model. These designations were applied to the wind turbines models and will be used for the remainder of the paper, based on their positions, as shown in Figure 1. Each turbine was also tested on its own at its respective position. The tunnel wind speed was held constant and the turbine RPM was varied to cover a range of tip speed ratios (λ).

2.5.2. Wind Farm Case

Here, both wind turbines were installed in the test section and the following procedures was followed. Firstly, power measurements were performed for the upstream wind turbine as a function of TSR -same with single wind turbine-, while the downstream wind turbine was operated at the fixed rotor speed , $\omega_{downstream} = 574\ rpm$. Then a tip speed ratio scan was performed for the downstream wind turbine by varying its rotational speed, with the upstream turbine was operated at the rated rotor speed, $\omega_{upstream} = 850\ rpm$. The tunnel wind speed was constant during these tests.

2.5.3. Calculations

For all cases, the turbine power coefficient, C_P, was calculated using equation (2)

$$C_P = \frac{P}{0.5\rho U_{pitot}^3 \pi (0.5D)^2} = \frac{\omega T}{0.5\rho U_{pitot}^3 \pi (0.5D)^2} \quad (2)$$

where P is the power, ω is the rotor speed, T is the torque measured by the shaft strain gauges and U_{pitot} is the uncorrected wind tunnel velocity, measured with the pitot tube.

The thrust coefficient, C_T, was calculated using equation (3)

$$C_T = \frac{Thrust}{0.5\rho U_{pitot}^2 \pi (0.5D)^2} \quad (3)$$

where $Thrust$ is derived based on strain gauge measurement at the tower base. Thrust data are only available for the upstream wind turbine.

3. Results

3.1. Pressure variation along the test section

Figure 4 shows the pressure drop along the free stream direction for a wind speed of 5.74 m/s for an empty test section. The pressure drop is less than 2 Pa in 16 m which is considered good.

3.2. Inflow velocity and turbulence intensity profiles

Figure 5 presents the velocity and turbulence intensity profiles in the empty wind tunnel test section at two locations: at the position of the upstream wind turbine and at the downstream wind turbine model. The measurements show a uniform streamwise velocity profile at both locations for $z/z_{hub} \geq 0.35$. The boundary layer on the tunnel floor grows with distance as expected.

Figure 5b presents the streamwise turbulence intensity profile TI_u (%) calculated at the positions of the upstream and downstream turbine models. The turbulence intensity at hub height is 1.88% for the upstream turbine model and 1.97 % for the downstream turbine model. Within the boundary layer height, δ i.e. z < 30 cm, TI_u values are higher (between 4% and 8%), again as expected.

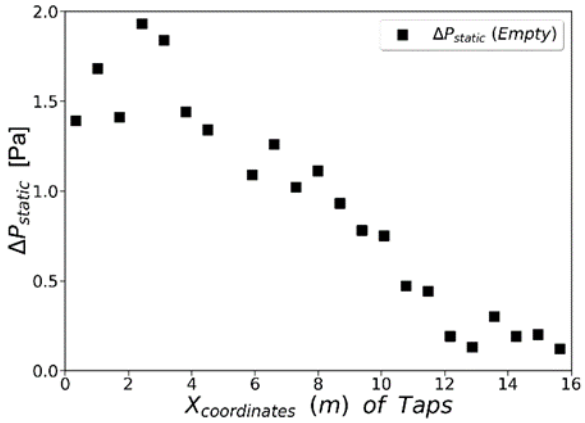

Figure 4. Pressure drop along the ceiling of the test section (in the streamwise direction) without wind turbine models in the wind tunnel test section

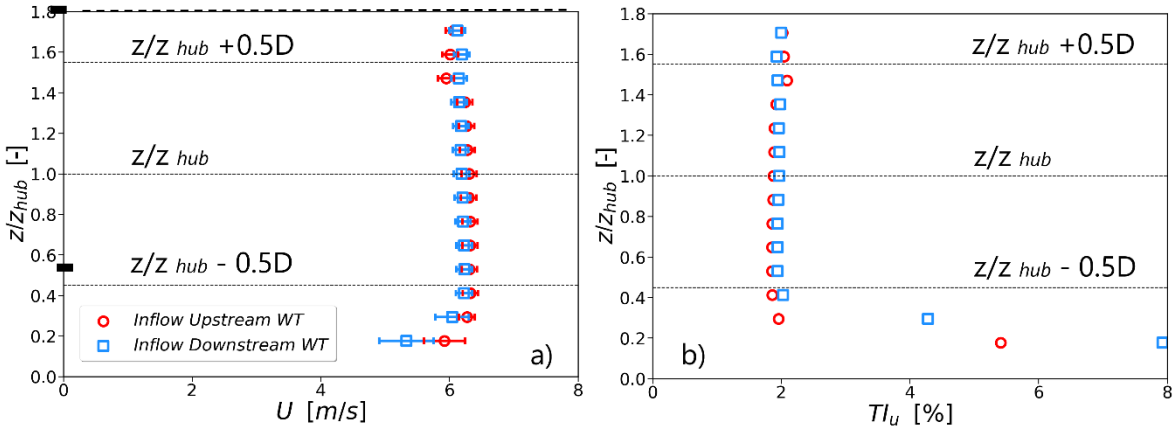

Figure 5. Vertical inflow profiles of a) streamwise velocity U (m/s) (error bars: standard deviation of streamwise velocity); and b) turbulence intensity, TI_u (%) in the empty wind tunnel test section, at the positions of the two wind turbine models.

Additional velocity measurements were performed at hub height, at two additional points in the lateral direction ($y = \pm 0.5D$) to examine the symmetry of the inflow streamwise velocity and the turbulence intensity at the locations of the two models, see Figure 6. A marginal asymmetry of the inflow profile and turbulence intensity at the location of the upstream profile appears to be diffused at the downstream turbine location.

3.3. Wind Turbine Performance

The performance of the two turbines was examined independently, i.e. when located on its own in the test section, see Figure 7. The Upstream WT was tested only at the upstream position, while the Downstream turbine was tested at both the upstream and the downstream positions. All results are very similar, suggesting the two turbines have very similar performance and that the turbine position in the wind tunnel does not affect performance.

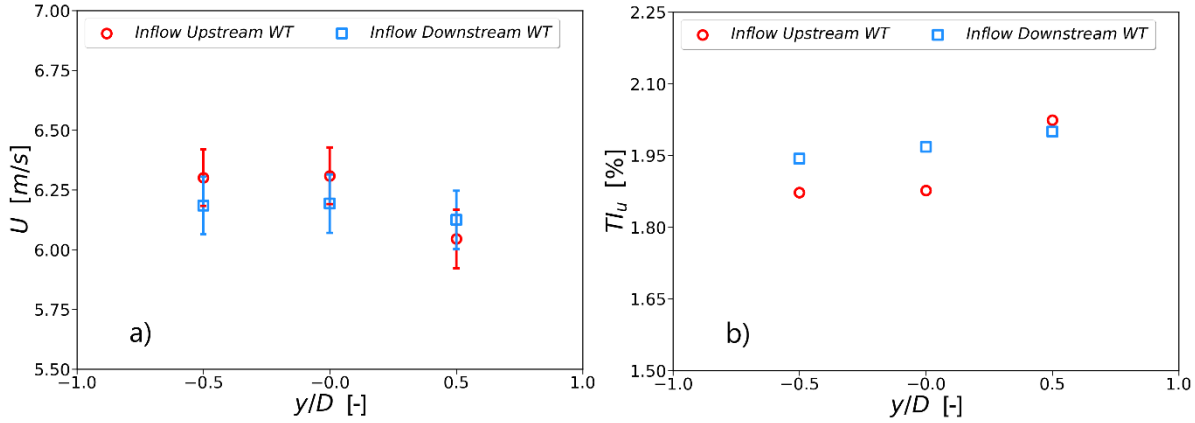

Figure 6. a) Streamwise velocity, u (m/s) (error bars: standard deviation of streamwise velocity) and b) Turbulence intensity, TI_u (%) variation along the spanwise direction in the empty wind tunnel test section, at the positions of the two wind turbine models.

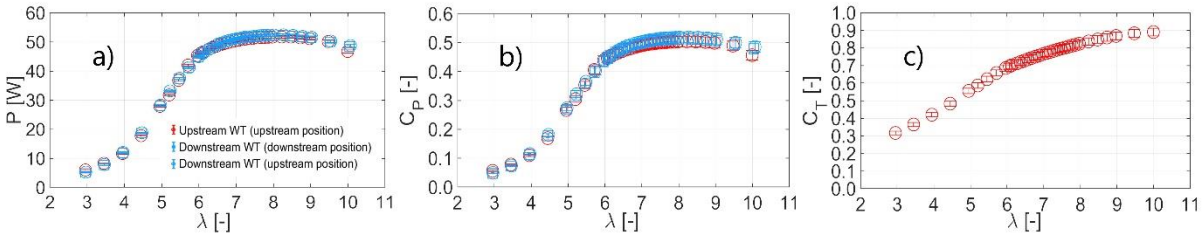

Figure 7. a) Power, P; b) power coefficient, C_P; and c) thrust coefficient C_T variation with tip speed ratio, λ, when each of the turbine models is placed independently in the wind tunnel test section. The downstream wind turbine model is measured at the downstream position (blue square) and also at the upstream position (blue circle). Error bars represent the measurement uncertainty of P, C_P and C_T.

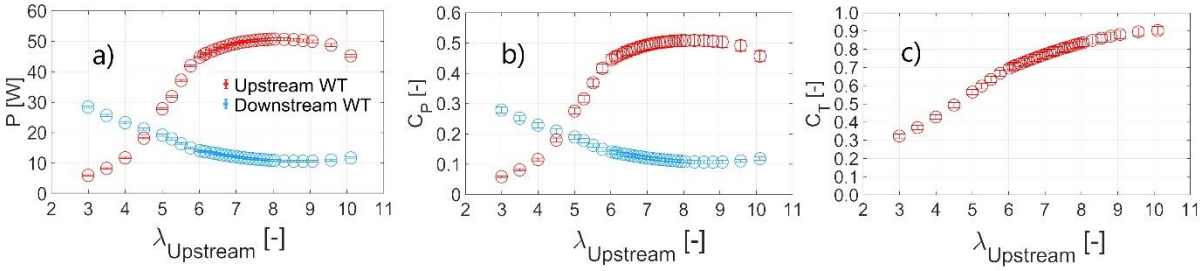

Figure 8. a) Power, P; b) power coefficient, C_P; and c) thrust coefficient C_T variation with upstream turbine tip speed ratio, $\lambda_{upstream}$, when both wind turbines are placed in the wind tunnel test section. The upstream wind turbine model rotates at variable rotational speed while the downstream wind turbine rotates at constant rotor speed (574 rpm, $\lambda_{downstream} = 5.86$). Error bars represent the measurement uncertainty of P, C_P and C_T.

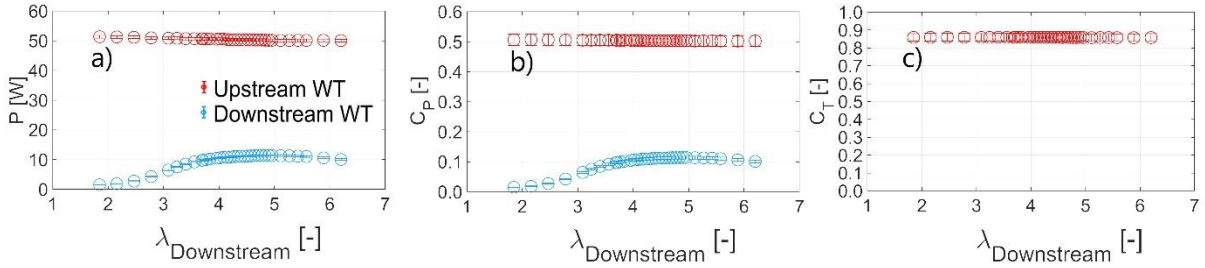

Figure 9. a) Power, P; b) power coefficient, C_P; and c) thrust coefficient C_T variation with downstream turbine tip speed ratio, $\lambda_{downstream}$, when both wind turbines are placed in the wind tunnel test section. The upstream wind turbine model rotates at constant rotational speed (850 rpm, $\lambda_{upstream} = 8.53$) while the downstream wind turbine rotates at variable rotor speed. Error bars represent the uncertainty in the measurement of P, C_P and C_T.

Figure 8 shows the performance of both turbines against $\lambda_{upstream}$, when the upstream and downstream turbines operate at variable and constant RPM, respectively. Clearly, the performance of the upstream turbine and the energy it extracts from the flow significantly affect the performance of the downstream one.

Figure 9 presents the performance of the two turbines when the upstream one operates at constant RPM and the downstream one operates at variable RPM. The upstream turbine remains largely unaffected while the downstream turbine displays peak performance at $\lambda_{downstream} = 5.1$.

The baseline case is considered that in which the upstream and downstream turbine operate at 850 RPM and 544 RPM, respectively, the tunnel wind speed is 5.7 m/s. For this case the expected performance is given in Table 1.

Table 1. Performance of the two wind turbines for the baseline case

	Rotational Speed	**Power**	**Power Uncertainty**	C_P	C_P **uncertainty**	C_T	C_T **uncertainty**
Turbine	RPM	[W]	[±W]	[-]	[±]	[-]	[±]
Upstream	850	44.6	0.45	0.50	0.02	0.88	0.02
Downstream	544	9.5	0.28	0.11	0.005		

4. Conclusions

The present paper discusses Phase I of the *Blind test on wind turbine wake modelling based on wind tunnel experiments*. Velocity, turbine performance and turbine load measurements are presented. All data are publicly available along with geometry and turbine data. It is envisaged that this phase will ensure all participants to the exercise are able to meaningfully simulate the flow past the two turbines and numerical solvers well prepared for the blind test on controlled wake modelling.

References

[1] Veers P, Dykes K, Lantz E, Barth S, Bottasso CL, Carlson O, et al. Grand challenges in the science of wind energy. Science (80-) 2019;366:eaau2027.
[2] Meyers J, Bottasso C, Dykes K, Fleming P, Gebraad P, Giebel G, et al. Wind farm flow control: prospects and challenges. Wind Energy Sci Discuss 2022;2022:1–56.
[3] Mühle F, Schottler J, Bartl J, Futrzynski R, Evans S, Bernini L, et al. Blind test comparison on

the wake behind a yawed wind turbine. Wind Energy Sci 2018;3:883–903.
[4] Kozmar H. Wind-tunnel simulations of the suburban ABL and comparison with international standards. Wind Struct An Int J 2011;14:15–34.
[5] Heckmeier FM. Multi-Hole Probes for Unsteady Aerodynamics Analysis 2022.
[6] Heckmeier FM, Breitsamter C. Aerodynamic probe calibration using Gaussian process regression. Meas Sci Technol 2020;31:125301.
[7] Mühle FV, Heckmeier FM, Campagnolo F, Breitsamter C. Wind tunnel investigations of an individual pitch control strategy for wind farm power optimization. Wind Energy Sci Discuss 2023;2023:1–31.
[8] Bottasso CL, Campagnolo F. Wind tunnel testing of wind turbines and farms. Handb Wind Energy Aerodyn 2022:1077–126.
[9] Campagnolo F, Castellani F, Natili F, Astolfi D, Mühle F. Wind Tunnel Testing of Yaw by Individual Pitch Control Applied to Wake Steering. Front Energy Res 2022;10:883889.
[10] Campagnolo F, Petrović V, Schreiber J, Nanos EM, Croce A, Bottasso CL. Wind tunnel testing of a closed-loop wake deflection controller for wind farm power maximization. J. Phys. Conf. Ser., vol. 753, IOP Publishing; 2016, p. 32006.
[11] Hansen MOL. Aerodynamics of wind turbines. Earthscan; 2008.